We are IntechOpen, the world's leading publisher of Open Access books Built by scientists, for scientists

6,900
Open access books available

185,000
International authors and editors

200M
Downloads

Our authors are among the

154
Countries delivered to

TOP 1%
most cited scientists

12.2%
Contributors from top 500 universities



WEB OF SCIENCE™

Selection of our books indexed in the Book Citation Index in Web of Science™ Core Collection (BKCI)

Interested in publishing with us?
Contact book.department@intechopen.com

Numbers displayed above are based on latest data collected.
For more information visit www.intechopen.com



Chapter

Exploitation of Bentonite for Wastewater Treatment

Kali Abderrahim, Loulidi Ilyasse, Amar Abdelouahed, Boukhlifi Fatima, Hadey Chaimaa, Jabri Maria and Mbarka Ouchabi

Abstract

Bentonite is a clay with interesting surface properties (affinity for water, adsorption capacity for electro-positive compounds ... .). The characteristics and clarifying properties of bentonite from various companies are the subject of numerous studies. The present work focuses on the study of the efficiency of bentonite and modified bentonite to purify aqueous solutions containing organic pollutants such as phenol. First, before starting the adsorption study, a physical–chemical characterization of the clay by FTIR, BET and XRD techniques was undertaken. The specific surface of the bentonite is calculated by BET. Then, the study of isotherms and kinetics of phenol adsorption on commercial BTC showed that this pollutant can be removed from liquid effluents with a significant percentage. Langmuir and Freundlich models were applied. Finally, the kinetic study performed by UV–Visible was reproduced by FTIR spectroscopy.

Keywords: bentonite, phenol, adsorption, FTIR, UV–Visible

1. Introduction

Bentonite is characterized by high adsorption, ion exchange, and swelling capacity, as well as by specific rheological properties (thixotropy). It, therefore, has wide applications, ever more numerous and in different fields (drilling, foundry, ceramics, painting, pharmacy, bleaching earth, ...). Bentonites play a significant role in a diverse range of environmental problems and their applications are steadily increasing. Among the few fields of application, bentonite can be used for the purification of gases [1], the elimination of radioactive elements [2, 3], the elimination of pesticides [4], and the elimination of phenol. This pollutant was removed by variety of clays and modified clay as the bentonite [5], the clinoptilolite [6], the composite of silica [7], the silica/hydrotalcite [8], the natural clay [9], the Montmorillonite, Clinoptilolite and Hydrotalcite [10], the hectorite [11], the untreated coffee wastes [12], the lignite [13], the zeolite X/activated carbon [14], the shells of eggs [15, 16] and the chitin/chitosan [16–18].

Zohra Dali and all [5] have studied the adsorption of phenol on two types of clays: sediment after chemical activation with ammonium chloride and bentonite which has undergone activation by sulfuric acid. They concluded that the acidified bentonite exhibits more affinity towards phenol with a limited adsorption capacity equal to 32.23 mg/g. Myroslav and al [6] studied the kinetics of phenol adsorption

on clinoptilolite modified by hexa decyl trimethyl ammonium (HDTAM). They have shown that phenol can be fixed by this clay with a percentage of (85–90%). The adsorption process is fast. All phenol were fixed after one hour. The adsorption isotherm is described by the Langmuir model.

By studying the interposed action of two kinds of clay (bentonite and kaolinite) by both the surfactant hexa decyl trimethyl ammonium (HDTAM) and the phenyl methyl ammonium bromide (PTMA), Uday and all [19], have shown that the kinetics of adsorption on both clays follows the model of the pseudo-second-order and the adsorption isotherm following the model Freundlich and Langmuir. The parameters thermodynamics shows that adsorption was exothermic and spontaneous. In another research, Jin and al [20], chose to intercalate a Na-montmorillonite with dihydroxy ethyl methyl ammonium bromide (ODEM). The results obtained showed that the adsorption kinetic of phenol by (Na-Mt) modified was pseudo-second-order. The adsorption isotherm described by the Langmuir model gave an adsorption capacity of (384.61 mg/g at 308 K). The parameters thermodynamics indicate that the adsorption process was exothermic and spontaneous. Richards and all [21], for their part, have studied the phenol adsorption kinetics on two clay (basaltic clay and bentonite) changes organically by hexa decyl trimethyl ammonium (HDTAM) and phenyl trimethyl ammonium. The results obtained shows that the adsorption kinetics of (HDTAM) -basaltic and (TMPA) -Bentonite was pseudo-second-order. For its part, Jianfeng and all [22] have studied the adsorption kinetics of phenol and ap-nitro-phenol and β - naphthol on organobentonite (Bentonite-TAB). They showed that phenol can be fixed by this organobentonite after 25 min at 69% and 92% for p-nitrophenol and 99% for β - naphthol. The treatment of phenol by adsorption flocculation using an organobentonite was studied by Yun Hwei [23]. The process consists of dispersing the bentonite in water by adding a cationic surfactant that has a short chain (BTMA). The result showed that BTMA bentonite had a high affinity for phenol and 90% of phenol was removed and 100% bentonite was recovered by the process of adsorption flocculation. The study by Basri and all [24] on bentonite modified by the surfactant cetyl trimethyl ammonium bromide (CTAB) as the adsorbent of phenol taking into account several parameters such as the pH of the solution, the contact time. At the initial concentration and temperature, we showed that the adsorption is maximal at pH = 9. The equilibrium was reached after 1 hour with a kinetic adsorption second order. The calculation of the thermodynamic parameter (ΔG°), enthalpy (ΔH°) and entropy (ΔS°) has shown that the adsorption on the organobentonite is possible spontaneous and exothermic in the range of temperature 0-40C °. The adsorption of phenol and 2-chlorophenol and 2,4,6 trichlorophenol by organo-clays (Na-montmorillonite) modified by transition metal complexes was undertaken by Boufatit and al [25]. The results showed that the adsorption capacity of organophilic clay is not obeyed in a logical order, but depends on the nature of the complex. The work carried out by SYuening and all [26] allowed the study of the elimination of phenol using Na-montmorillonite modified with two new Gemini surfactants containing hydroxyl groups, 1,3-bis (hexa decyl dimethyl ammonio) -2-hydroxy-dichloride (BHHP) and1,3-bis (octyl dimethyl ammonio) -2-hydroxy-dichloride (BOHP) as adsorbent. The effects of contact time, pH, temperature, and concentration of adsorbate on the adsorption performance of phenol by the Na - modified montmorillonite were examined by tests in batch. The results have shown that the kinetics follows the pseudo-second-order model, and the adsorption equilibrium data are described by the Langmuir model. The thermodynamic study has shown that the adsorption of phenol is a spontaneous and exothermic process.

The present chapter is interested in the study of the elimination of phenol as a very toxic pollutant using commercial bentonite (BTC) and treated bentonite. The treatment of the clay was carried out with acid solutions of different concentrations.

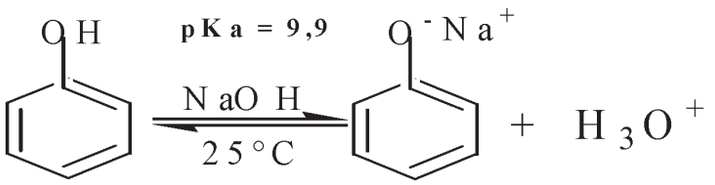
Before starting the pollution treatment, physicochemical characterization of the bentonite was undertaken. The elimination of the pollutant was carried out by studying kinetic and isothermal adsorption process.

2. Materials and methods

2.1 Presentation of the phenol used

In the form of white crystals at ambient temperature, it is of GMBH origin. It has a purity of 99.5%. Phenol solutions were prepared with distilled laboratory water. The main characteristics of phenol are grouped in **Table 1**.

Phenol is weakly acidic and transforms in a basic medium into a phenolate anion according to the reaction:



Phenol is very toxic: VA = 19 mg.m $^{-3}$.

2.2 Procedure

The various phenol adsorption experiments on bentonite are carried out at room temperature. A fixed mass m_0 = 0.1 g of bentonite is contacted with the aqueous solution of phenol with an initial concentration of $C_0 = 2.10^{-3}$ M. The mixture is then stirred at 500 rpm for an adsorption time t (tads). For each experiment, the solution pH is adjusted, as necessary, by the addition of HCl (0.1 N) or NaOH (0.1 N).

After the time required for adsorption (tads), the solutions are filtered through a 0.45 μm microporous membrane, and then the filtrates obtained are analyzed by UV/Visible spectrophotometry and the bentonite by IRTF spectrophotometry.

Commercial bentonite (BTC) was treated with HCl 3 N (BTC3N) and HCl 12 N (BT12N) overnight. The objective of these treatments is to determine the effect of acid on the capacity of adsorption by BTC. The study of the adsorption kinetics of phenol and its isotherms was carried out by UV / visible and IRTF.

2.3 Spectroscopic techniques for characterization and analysis

2.3.1 IRTF and UV/visible spectrophotometry

IR and UV / Visible spectrophotometry are two analysis techniques, based on the principle of absorption by the sample of a beam in IR [400–4000] cm^{-1} or UV / Visible [200–800] nm range.

TF (temperature of melting in °C)	TE (temperature of boiling in °C)	S/H_2O (gL $^{-1}$) (20 °C)	μ (D)	pKa (acidity constant)
41	181	93	1.59 (pH → OH)	9.9

Table 1.
Characteristics of the phenol used.

- **Spectrophotometer IR** is Fourier transform (FTIR) of the JASCO 4000, provided with a sensor (TGS) and a source ceramic, separated by an optical system using an interferometer Michelson. The operating conditions for analysis are as follows: - Resolution: 2 or 4 cm^{-1} - Initial beam intensity: 22000 - Analysis range: 400–4000 cm^{-1}. The solid samples to be analyzed are diluted to 4% by weight of the material in KBr, then finely ground. A mass of 50 mg (48 mg of KBr + 2 mg of BT) was placed in a mold and then subjected to a pressure of 6 tones.

- **UV / visible spectrophotometer**, with a double beam allows the recording of spectra between 200 nm - 800 nm. This technique is generally used for quantitative analysis. We used it for the determination of the quantities of residual phenol, not adsorbed on the bentonite.

2.3.2 SEM/EDX scanning electron microscopy

Scanning electron microscopy is a spectroscopic technique, based on the principle of electron-matter interaction. An electron beam scans the surface of the powdered solid, deposited on a sample holder, which in response re-emits certain particles (electrons). Different detectors make it possible to analyze these particles and fully reconstruct the image or cartography of the surface of the solid analyzed. Combined with the EDX technique, it provides access to the chemical composition of the solid. This technique is used for the characterization of the texture of bentonite and its chemical composition.

3. Results and discussions

3.1 Physical-chemical characterization of raw and treated bentonite

Commercial bentonite (BTC) in the form of a very fine white powder was purchased from Rhône Poulenc. Its origin is a volcanic clay rock, strongly colloidal. It is identical to montmorillonite of the smectite group, consisting mainly of alumina silicate. Its crystalline structure is in the form of a sheet of alumina octahedron, placed between two sheets of silica tetrahedron. The percentage of silica is 50 to 60% and that of alumina is between 15 and 20%, the rest is in the form of metal oxides (Fe, Mg, Ti) and oxides of alkaline elements and alkaline earth (Na, K, and Ca) [3]. The amount of interstitial H_2O and the nature of the exchangeable cations present in the interleaf space determine the Physico-chemical properties of bentonite. These essential properties enhance bentonite in its field of use and application.

Before performing the phenol removal experiments, the commercial bentonite BTC and treated with 3 N and 12 N HCl acid were characterized by the techniques of BET, IRTF, and SEM / EDX to evaluate the surface and active functions of clay.

3.1.1 Characterization by the BET method

The specific surface of the bentonite was evaluated at 19 m^2/ g by the BET method using an automatic device of the ASAP type from the European Institute of Membranes (IEM) in Montpellier. **Figure 1** shows the adsorption/desorption isotherm of N_2 at −196° C on the solid and in the **Table 2** the parameters characterizing its texture. The isotherm thus obtained is of type IV, according to the IUPAC classification, exhibiting a hysteresis characteristic of mesoporous solids of type H_3.

For BTC 3 N and BTC 12 N, the specific surface areas are equal to 96 m^2/g, greater than the surface area of BTC, indicating an increase in nitrogen adsorption sites.

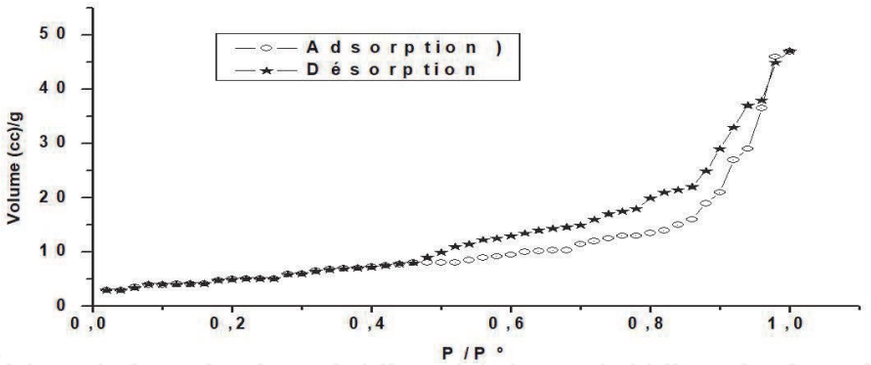


Figure 1.
Adsorption/desorption isotherm of N_2 on bentonite.

Methods	Values	Units
Point B method	18.5351	Specific area (m^2 / g)
BET	19.4377	
BJH adsorption	20.2408	
BJH desorption	28.9052	
BET	0.058366	Volume (cm^3 / g)
BJH adsorption	0.070829	
BJH desorption	0.072696	
BET	120.1091	Diameter (Å)
BJH adsorption	139.9721	
BJH desorption	100.5997	

With BJH indicates pore size.

Table 2.
Textural characteristics of bentonite.

For many technical applications, raw bentonites must be subjected to a preparation adapted to the requirements of their use (activation). Activation with acids such as hydrochloric acid increases porosity by the peripheral dissolution of Smectites. This results in a product with a high adsorption capacity. They are used for clarification or protein stabilization operations in musts and wines [27].

3.1.2 Characterization by SEM/EDX

Scanning electron microscopy images, taken at different scales and two different locations, under the energy of 30 keV, are shown in **Figure 2** for BTC, BTC 3 N, and BTC 12 N. They show that BTC is not treated with HCl, which has a mesoporous sheet structure and variable particle size. Their values are in perfect agreement with the results of BET and BJH. On the other hand, for treated BTC, the SEM images show an increase in the number of pores and a decrease in their size with the concentration of HCl. The surface of BTC 12 N becomes very compact indicating the formation of several micro-pores.

3.1.3 Characterization by IRTF

The IR spectrum of **Figure 3** shows the absorption bands of commercial bentonite before its contact with phenol. The bands thus observed are characteristic of

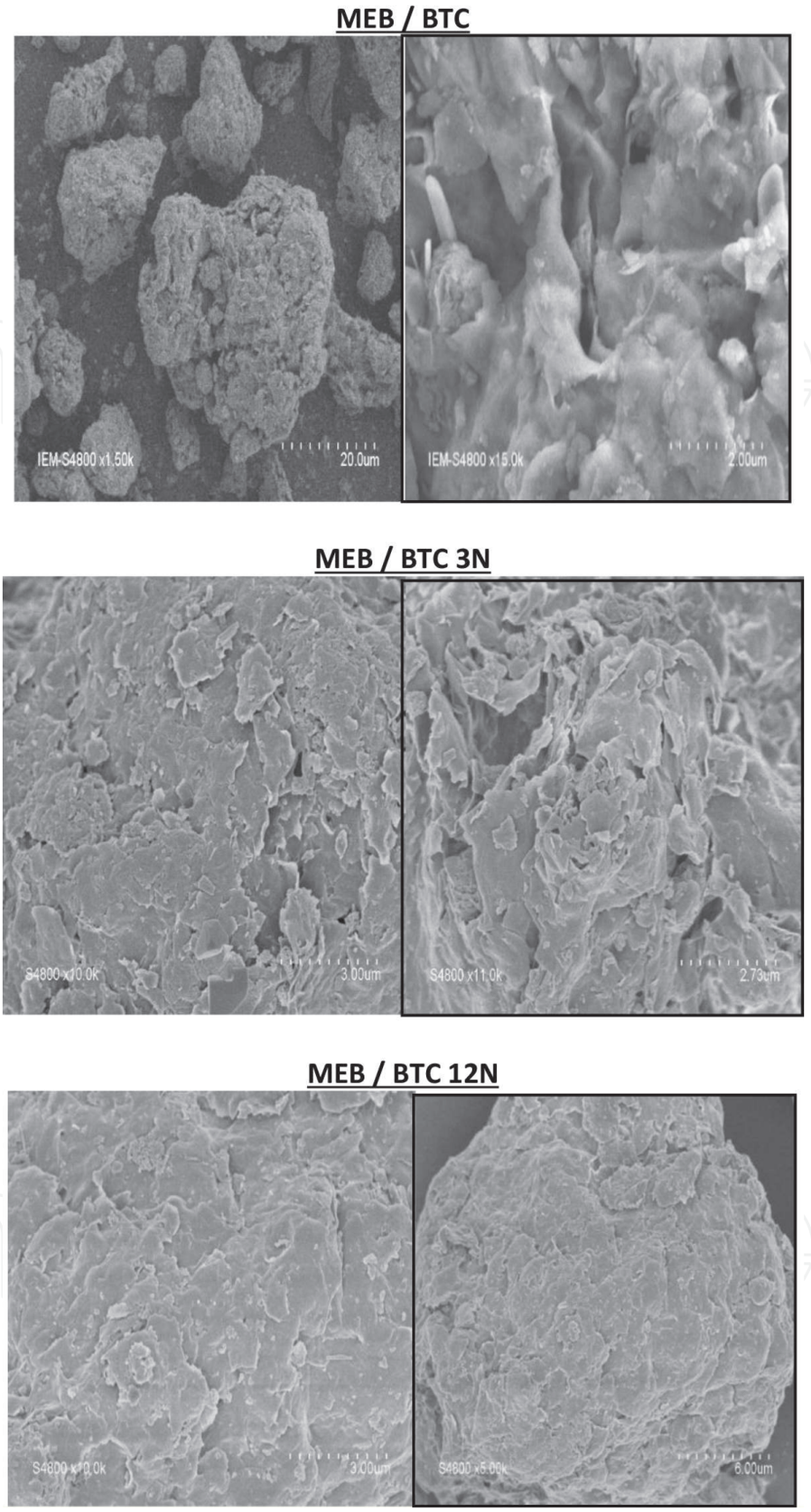


Figure 2.
Microscopic images of BTC, BTC 3 N, and BTC 12 N.

the structure of clays belonging to the smectite class, such as montmorillonite and bentonite. **Table 3** shows the different frequencies and their attributions to the different vibration modes [28, 29].

The comparison between raw and treated bentonite has been illustrated in **Figure 4**. This figure represents a comparison of the IR spectra of the three samples:

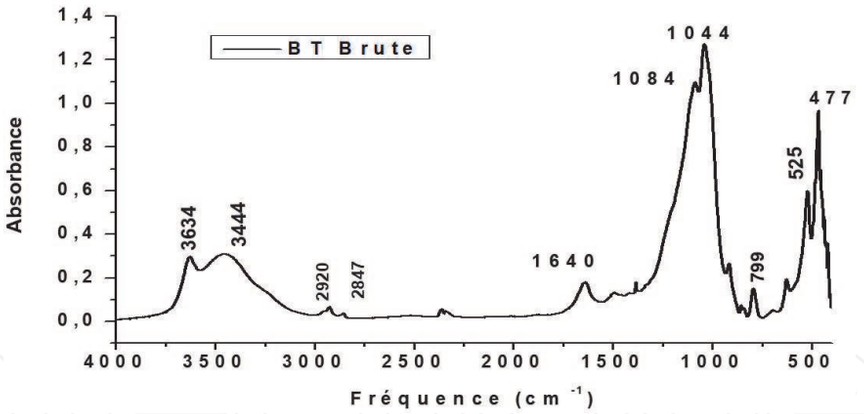
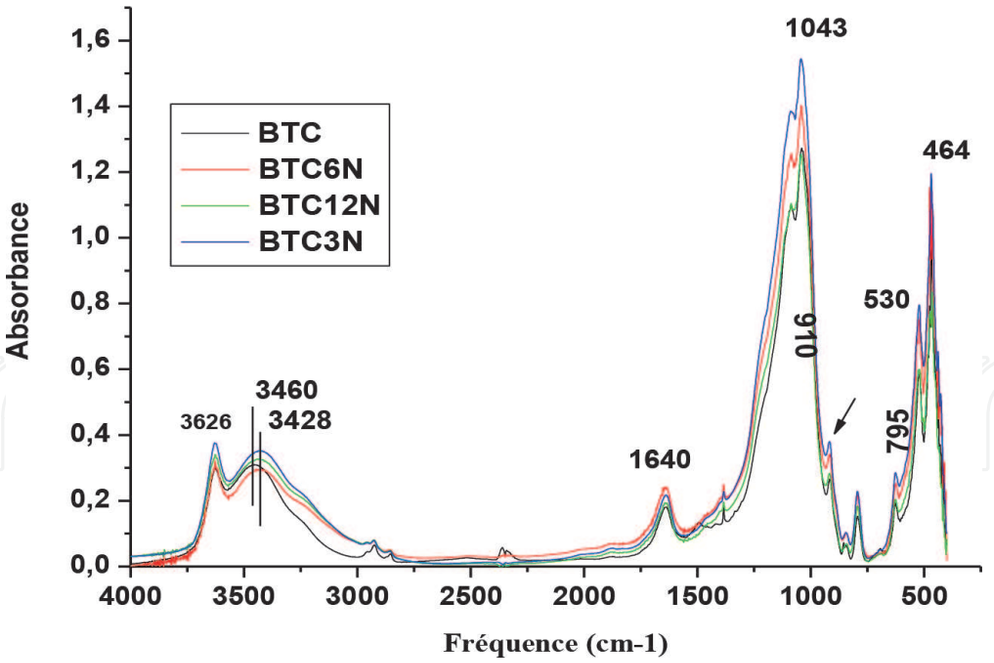


Figure 3.
IRTF spectrum of commercial bentonite.

ν (cm $^{-1}$)	Vibrations	Vibration type
477	Si-O-Si	vibration of distortion out of plane
525	Si-O-Al or Mg, Fe	vibration of distortion out of plane
630	Al-O and Si-O	vibration of distortion out of plane
795	Quartz	Si-O vibration
845	Al-Mg-OH	Vibration of valence
875	Al-Fe-OH	The vibration of valence (Al; Mg)
917	Al- AlO -H	The vibration of valence OH (Fe, Mg)
1035	Si-O- Si tetrahedron	Asymmetric vibration in the plane
1084	Al-OH	Vibration in the plane
1494	OH (H_2O)	H_2O deformation vibration
1640	CH_2: alkanes	The vibration of deformation CH bond of
2920 2847	H_2O	H bond or of combination (2x1640)
3252	Interfoliar H_2O	Asymmetric and symmetrical vibration
3444	Si-OH; Al-Al-OH	Free OH elongation vibration
3634		

Table 3.
IR bands of commercial bentonite.

BTC, BTC 3 N, and BTC 12 N, before adsorption of the phenol. It can be observed that the acid treatment of BTC with 3 N HCl leads to a slight increase in the bands initially identified on BTC in the [3700–1600] cm^{-1} domain compared to BTC 12 N and BTC 6 N. However, in the [400–1500] cm^{-1} domain, this evolution is not observed since the intensities of the bands decrease in the following order: BTC 3 N > BTC 6 N > BTC 12 N, the treatment of alumino-silicates with concentrated acids generates a change in the Si / Al ratio, the major element in the composition of bentonite and on the occasion of new MO bonds (M: Al, Si, or Mg) of the same type as those characterized for BTC can appear and contribute to the increase of these intensities. These bonds (MO) can combine in an acidic medium with the H^+ protons to form hydroxyl groups, which would explain the increase in the band at 3630 cm^{-1} (isolated or terminal OH). The increase in the band at 3435 cm^{-1}, linked to the interfoliar H_2O, may be due to its adsorption and that at 3252 cm^{-1} to the strengthening of the hydrogen bond between water and OH groups [28].



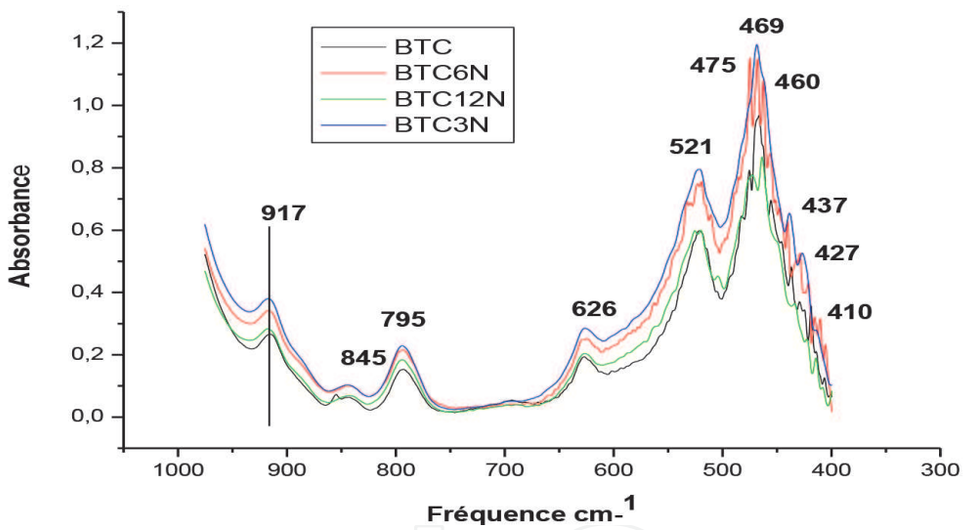


Figure 4.
IR spectra of BTC, BTC 3 N, and BTC 12 N.

On the other hand, these results are in good agreement with the increase in the specific surface which goes from 19 m^2 /g for BTC to 96 m^2/g for BTC 3 N and BTC 12 N.

3.2 Kinetics study of phenol adsorption on bentonite

3.2.1 Study by UV/visible spectrophotometry

3.2.1.1 Adsorption kinetics of phenol on BTC

The phenol adsorption kinetics were studied on commercial bentonite (BTC) and bentonite had undergone treatment for 12 hours with 3 N HCL (BT3N) and 12 N HCl (BT12N). To determine the time necessary for obtaining the adsorption equilibrium, phenol adsorption experiments ($C_0 = 2.10^{-3}$ M) were carried out for different contact times with a mass m = 0.1 g of commercial and treated bentonite.

It can be observed from the UV spectra of the residual phenol in **Figure 5**, the presence of two peaks of phenol, successively at max = 210 nm and 270 nm. Their position does not change concerning that of the pure phenol, which indicates that there is no reaction in solution between the phenol and the species released by the bentonite. The presence of two shoulders at λmax = 230 nm and λmax = 287 nm, is linked to the formation of the phenolate anion, which is favored in a basic medium. An increase in the pH value of the solutions from 8.9 to the value 10, which is equal to the pKa of phenol, was recorded for the stirring times. This increase in pH is explained by the release of the basic species by the BTC, in particular the Na^+ cations.

On the other hand, the intensities of the peaks gradually decrease with the contact time, which indicates that the adsorption of phenol on BTC is favored in a basic medium.

By taking into account the deconvolution of the spectra, the exact intensities of the two peaks can be determined. The residual concentration of phenol Cr is in this case represented by the maximum absorbance of the first peak (Ar) in the calibration curve. This will allow the determination of the amount of phenol adsorbed Cards for different contact times using (Eq. (1)), namely:

$$C_{ads} = \frac{C_0 - C_r}{m_{BT}}.M.Vsol = \frac{(A_0 - A_r)}{m_{BT}}.M(phenol).Vsol \quad (mg/g) \qquad (1)$$

where A_0 is the maximum absorbance of the peak at 270 nm for a concentration of phenol alone ($C_0 = 2.10^{-3}$ M; $A_0 = 2.71$). The use of the above spectra leads to the phenol adsorption kinetics curve given in **Figure 6**. This curve shows that the adsorbed quantity of phenol rises rapidly as a function of time (t < 5 h) and then keeps a practically constant value for longer times. The saturation value of the

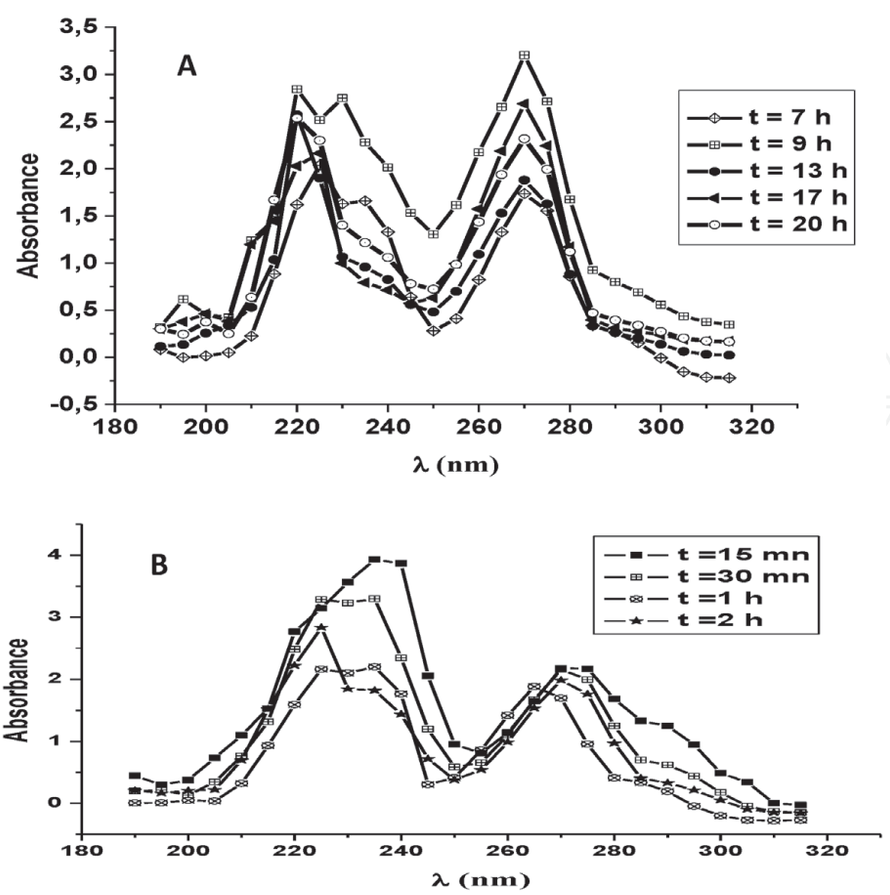


Figure 5.
(A and B) Evolution of the residual concentration of phenol after different adsorption times on bentonite.

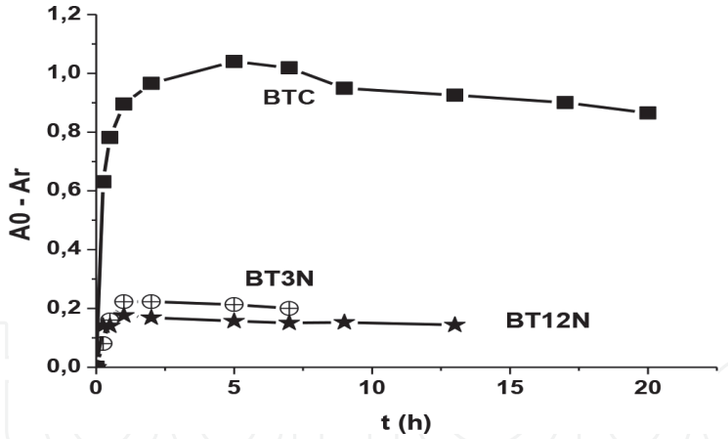


Figure 6.
Adsorption kinetics of phenol (Co = 2.10^{-3} M) on BTC / BTC3N / BTC12N.

surface corresponds to a concentration of the adsorbed phenol Cad = 8.10^{-4} M, which indicates, for C $_0$ = 2.10^{-3} M, a rate of elimination of the phenol of 40%. The linear rise observed may indicate the adsorption of phenol on equivalent sites, and the plateau obtained reflects a limited number of adsorption sites.

The same evolution is observed for the adsorption of phenol on BT3N and BT12N with a significant drop in the quantity of phenol adsorbed at saturation. The acid treatment of BTC resulted in a significant loss of adsorption sites (**Figure 6**), following the results of SEM analysis, which showed a significant decrease in the pore size of the solids treated, which prevents access to the solids adsorption sites.

3.2.1.2 Kinetic models

To elucidate the process of adsorption of phenol on BTC, several kinetic models have been proposed by Lagergren et al. [30], Ho et al. [31] and Boukhlifi et al. [32, 33] by considering pseudo-first–first-order and pseudo-second-order kinetics. The results obtained in this work can be subject to equations resulting from these models [30–33].

3.2.1.2.1 Pseudo first-order kinetics

Either phenol adsorption reaction on BTC:

$$\mathrm{Ph} + * \leftrightarrow \mathrm{Ph}*\,(\mathrm{Ph} = \text{phénol})$$
$$\mathrm{C_r}\ (\mathrm{S_0} - \mathrm{S})\ \mathrm{S}$$

Cr: residual concentration of phenol, S and S_0 are, respectively, the area occupied by phenol and the total area of BTC.

The differential equation that results from the adsorption reaction is as follows (Eq. (2)):

$$\frac{dS}{dt} = K_1.C_r.(S_0 - S) \Rightarrow \frac{dq_t}{q_e.dt} = K_1'.\left(1\text{-}\frac{q_t}{q_e}\right) \qquad (2)$$

where qt, in (mg / g) is the amount of phenol adsorbed at t; QE, in (mg / g) is the quantity of phenol at adsorption equilibrium and K '(min^{-1}), the pseudo-rate constant.

Using the initial conditions (at, t = 0; qt = 0) and (at, t; qt), its rearrangement after integration gives (Eq. (3)):

$$\ln\left(q_e - q_t\right) = \ln q_e - k_1'.t \tag{3}$$

The plot of ln (qe - qt) as a function of a (t), given in **Figure 7**, does not lead to a straight line as provided by the model equation. The curve obtained from the experimental data seems rather formed of two portions of straight lines. The first before t = 5 h (**Figure 7**) of negative slope can conform with the kinetic model of pseudo-first-order where the adsorption of phenol occurs in a very fast way (kinetic figure). However, the second portion, with a positive slope (**Figure 7**), is in contradiction with the equation of the proposed model. The linear regression coefficients R^2 of the two lines are not close to 1, which makes it possible to conclude that the kinetics of adsorption of phenol on BTC cannot be described by a pseudo-first-order speed. In addition, the calculated value of qe (qe = 47 mg / g) is much higher than the experimental value (≈14.5 mg / g).

3.2.1.2.2 Pseudo second order kinetics

The same treatment can be carried out for the pseudo-second-order kinetics (Eq. (4)), namely:

$$\frac{dq_t}{dt} = k_2'.\left(q_e - q_t\right)^2 \Rightarrow \frac{t}{q_t} = \frac{1}{K_2'.q2_e} + \frac{1}{q_e}.t \tag{4}$$

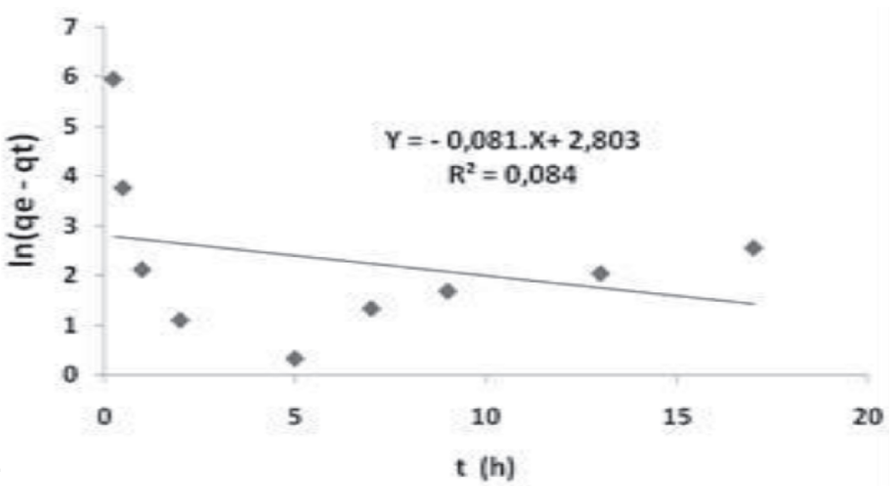


Figure 7.
Kinetics modeling according to the pseudo-first-order model ln (q_e - q_t) as a function of a (t).

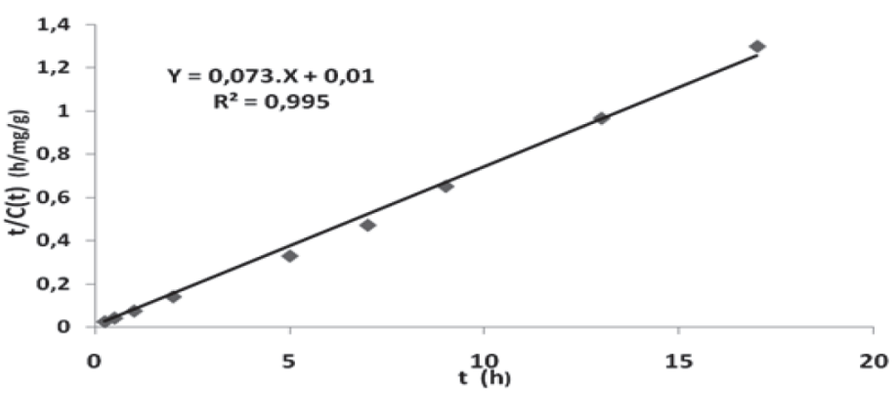


Figure 8.
Kinetics modeling according to the pseudo second order model t/qt = f (t).

The application of this equation to the experimental result of **Figure 8**, leads in this case to plotting t / qt = f (t)) to the right of **Figure 8**, with a linear regression coefficient (R^2 = 0.995) very close to 1. The parameters K′2 and qe, determined from the slope (1 / qe) and the y-intercept (1 / $K'_2.qe^2$) of the equation of the line, are respectively equal to 0.532 g / (mg.h) and 13.7 mg / g. The value of qe obtained is in perfect agreement with the experimental value (≈14.5 mg / g), which indicates that the adsorption of phenol on bentonite obeys pseudo-second-order kinetics for the entire time range studied.

3.2.1.2.3 Intra-particule diffusion model

The diffusion phenomenon (adsorbate ⇒adsorbent) also plays a determining role in the adsorption kinetics. The equation resulting from the treatment of the intra-particle diffusion model is given by the following relation (Eq. (5)) [34–36]:

$$q_t = K_d.\sqrt{t} + C \quad (5)$$

where Kd is the intraparticle diffusion constant and C a constant. In the case where C = 0, the intra-particulate diffusion step is the step that controls the adsorption process, if C is nonzero this step is not limiting.

The plot $q_t = f(\sqrt{t})$ leads to the curve of **Figure 9**, made up of two phases: the first increasing for low contact times (t < 5 h) and the following decreasing for longer times. The line corresponding to the first phase shows that C = 7.276 ≠ 0 and Kd = 5.087 mg / (g.h1 / 2). This result is not adapted to the hypothesis of the model on C and consequently, the diffusion process is not limiting.

3.2.2 Study of phenol adsorption on raw and treated bentonite by IR spectrophotometry

The masses of the solids resulting from the BTC/phenol contact were analyzed by IRTF. **Figure 10** shows the evolution of the spectra obtained after t = 1 hour and 17 hours of contact. The overall analysis of these spectra shows a clear decrease in the absorption bands of BTC, located at 477, 525, 1035, 1084, and 3634 cm^{-1} and related to the vibrations of the M-O bonds where M can represent the atoms of Si, Al, or Fe (**Table 2**). The decrease in these bands can be explained by their direct

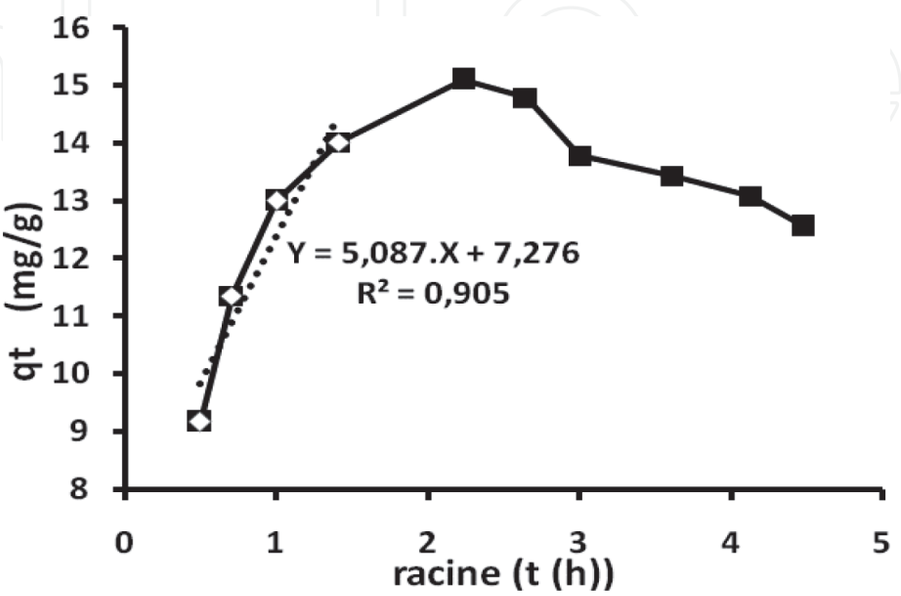


Figure 9.
Intra-particle diffusion model.

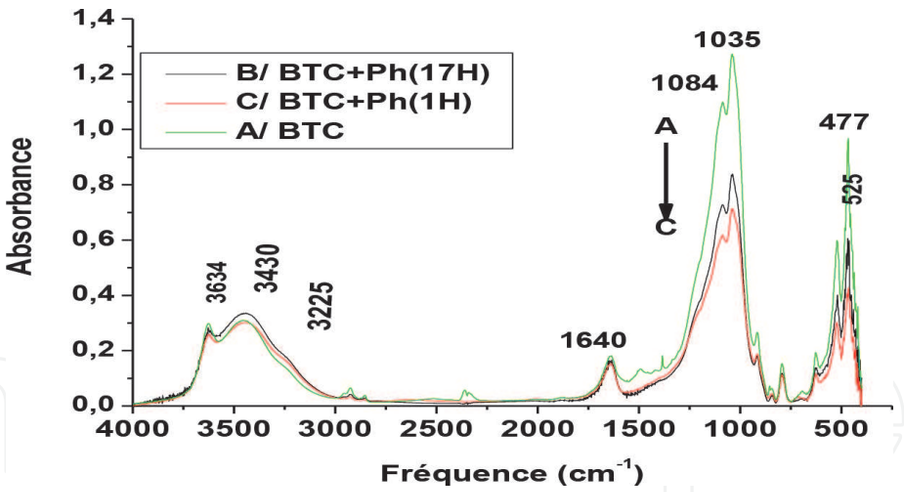
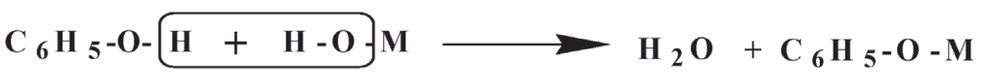


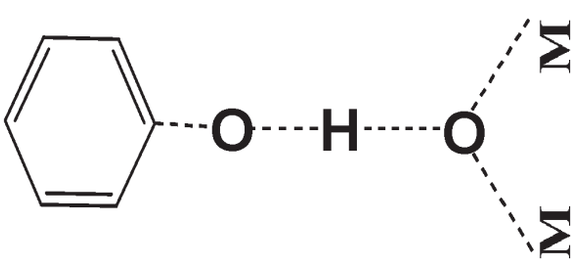
Figure 10.
IR spectra of phenol adsorption on BTC.

involvement in the adsorption of phenol on different sites of BTC. Their positions, which remain unchanged, meaning that the adsorption of phenol occurs at superficial sites. Indeed, for these two contact times, the intensities of these bands are practically equal, following the quantities of the adsorbed phenol, determined previously (**Figure 6**).

On the other hand, the bands located at 3430 and 1634 cm^{-1}, attributed to the OH vibrations of the interfoliar water and the shoulder at 3225 cm^{-1}, attributed to the OH group linked by the hydrogen bonds (H ... OH), increase slightly in intensity. For the first band, there is probably the formation of interfoliar water by dehydroxylation and for the last band, the formation of hydrogen bonds during the adsorption of phenol. The formation of H_2O during the adsorption of phenol on clay solids have already been mentioned by several authors according to the following process:



This proposition is in good agreement with our results which simultaneously show the increase in the H_2O bands and the decrease in the vibration band of the O -H groups at 3634 cm^{-1}. Moreover, the mechanism of adsorption of phenol by hydrogen bonding has also been mentioned by SYuening and al [26]. This bond, characterized by the band at 3225 cm^{-1}, results from an interaction between phenol and the oxygen atoms of the surface. It appears more marked for t = 17 h than t = 1 h of adsorption, following the intensities of the OH (3636 cm^{-1}) and interfoliar H_2O (3430 cm^{-1}) vibration bands.



Adsorption of phenol on bentonite treated with 3 N and 12 N HCl was also monitored by IR. The spectra obtained are illustrated in **Figures 11** and **12**. It can be

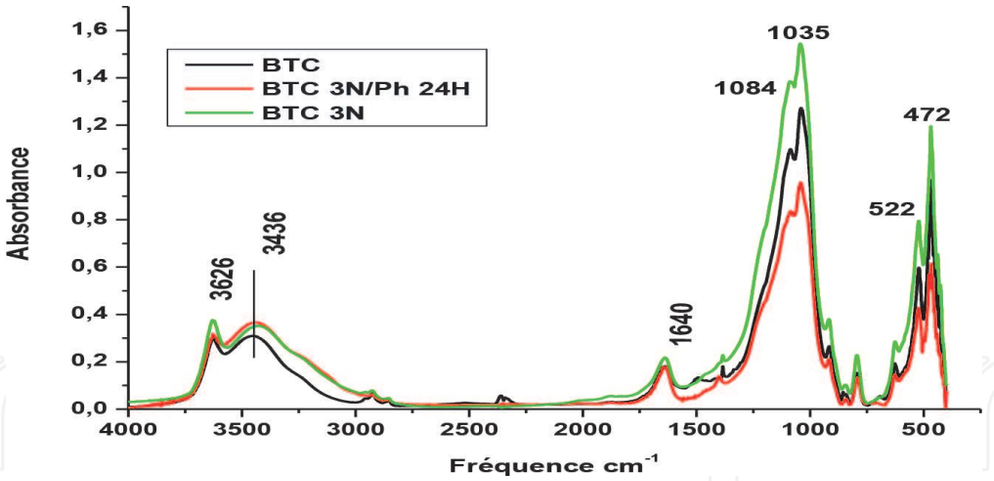


Figure 11.
IR spectra of phenol adsorption on BTC 3 N.

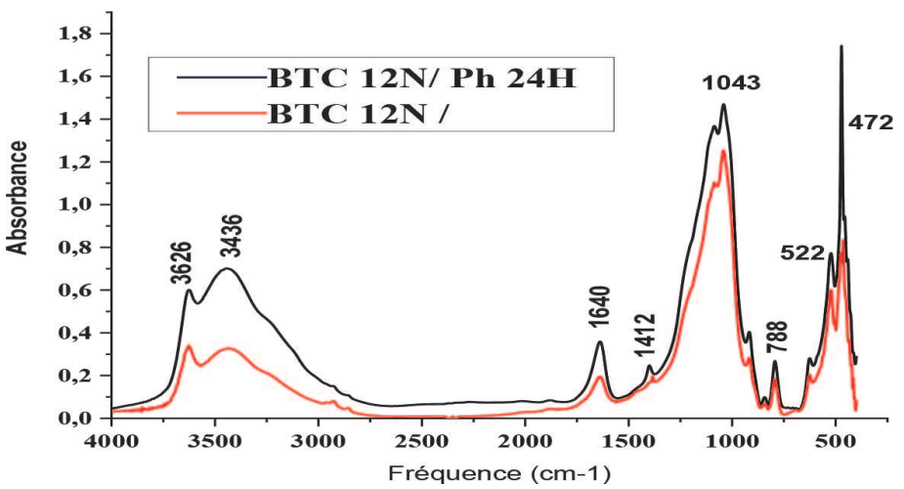


Figure 12.
IR spectra of adsorption of phenol on BTC 12 N.

noted first that the bands detected on BTC (spectrum A) are also observed at the same positions on BTC 3 N (spectrum B) with an increase in their intensities. This means that the acid treatment leads, in the range [300–1100] cm^{-1}, to the creation of MO bonds of the same type as those observed in BTC (Metal: Si, Al, and Fe) probably by breaking the OMO bonds or MOM. This explanation is confirmed on the one hand, by the increase in the intensity of the band to 3626 cm^{-1}, often attributed to the vibration of the MOH (free OH) bond and on the other hand, by the increase in the specific surface area which goes from 19 m^2 / g for BTC to 96 m^2 / g for BTC 3 N. The band at 3436 cm^{-1}, linked to the formation of the hydrogen bond increases in intensity under the effect of the acid treatment of BTC.

Furthermore, the adsorption of phenol on BTC 3 N leads to a reduction in the intensities of the characterized bands, except for the bands located at 3436, 3225, and at 1640 cm^{-1}. Taking into account the kinetic curve of **Figure 6**, it was found that the amount of phenol adsorbed by BTC 3 N is lower than that adsorbed by BTC.

3.3 Isothermal study of the adsorption of phenol

The adsorption isotherm was obtained at T = 25° C, by bringing different initial concentrations of C_0 of phenol into contact with BTC for a period t = 5 hours at

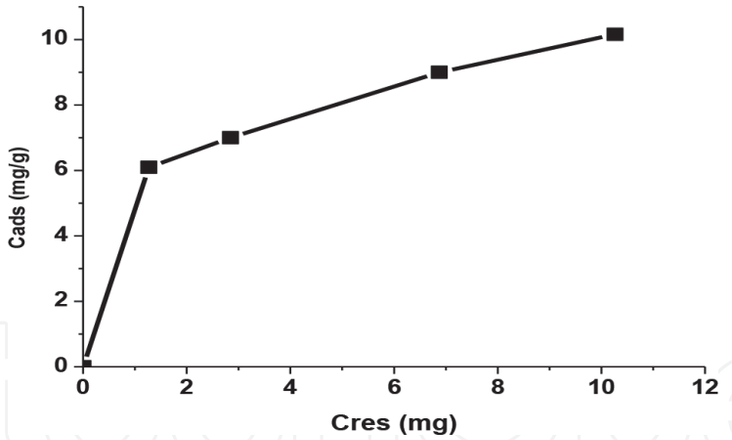


Figure 13.
Phenol adsorption isotherm.

pH = 6. The study of this isotherm is essential since it makes it possible, from known models, to obtain information on the adsorption parameters characterizing the adsorbate/adsorbent interaction.

The plot of the amount of adsorbed phenol (Cads) as a function of Cr gives the curve of the corresponding isotherm, represented by **Figure 13**. Several models are used to exploit the adsorption isotherms, the most commonly adapted to the adsorption of liquids are the isotherms of Langmuir (homogeneous sites) and Freundlich (heterogeneous sites). The latter is used to determine the parameters giving information on the nature of the interaction (adsorbate/adsorbent).

3.3.1 Langmuir model

This model assumes that the adsorption sites are energetically equivalent and there is no interaction between the adsorbates at two neighboring sites. The equation that governs this model is as follows (Eq. (6)):

$$q_e = \frac{Q_{max}.b.C_e}{1 + b.C_e} \tag{6}$$

Its linearization makes it possible to determine the constants Qmax and b (Eq. (7)), namely:

$$\frac{1}{q_e} = \frac{1}{b.Q_{max}} \cdot \frac{1}{C_e} + \frac{1}{Q_{max}} \tag{7}$$

It can be observed in **Figure 14** that the experimental results do not verify the Langmuir model since the plot of 1 / qe = f (1 / Ce) does not give a straight line. Besides, the theoretical line obtained by linear regression of the experimental points gives a correlation coefficient R^2 = 0.938, less than 1. The constants Qmax and b deduced from the ordinate at the origin and the slope of this line are, respectively, equal at Qmax = 10.42 mg / g and b = 1.05 m/g. Another parameter noted RL given by the relation below (Eq. (8)), characterizes a constant of the equilibrium of the Langmuir model. It makes it possible to predict whether such a model is favorable or not according to certain conditions on the values of RL:

$$R_L = \frac{1}{1 + b.C_0} \tag{8}$$

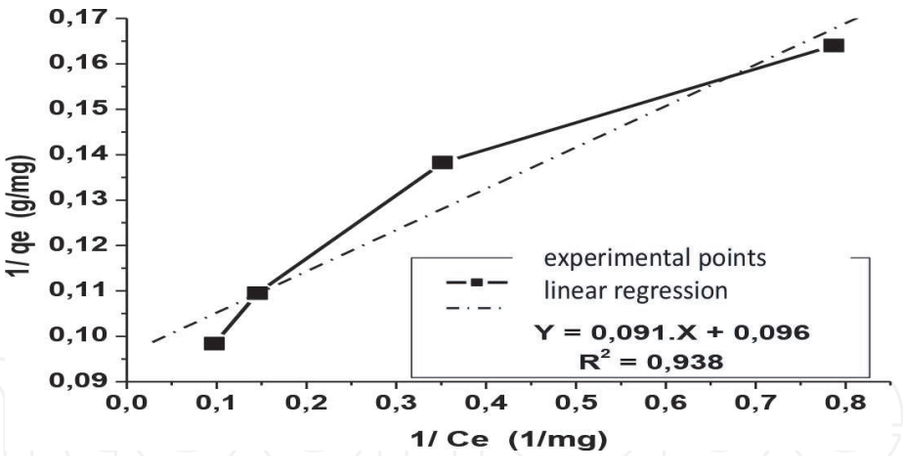


Figure 14.
Langmuir isotherm for the adsorption of phenol on BTC.

If 0 < RL <1: the isotherm is favorable; if RL = 1: the isotherm is linear and if RL > 1: the isotherm is not favorable and if RL = 0: the isotherm is irreversible.

The calculation of RL is carried out for C0 (max) = 6.10-3 M = 11.28 mg, which gives for RL a value of 0.08. This value is very close to 0 if one takes into account the uncertainties on b and C0, which confirms that the Langmuir model is not favorable.

3.3.2 Freundlich model

This model is often applied in liquid / solid adsorption, it takes as the main assumption a heterogeneity of the solid adsorption sites. The empirical equation established by Freundlich is as follows (Eq. (9)):

$$q_e = K_F.C_e^{1/n} \tag{9}$$

where K, $_F$, and n are the Freundlich constants, related, respectively, to the adsorption capacity and its intensity. Applying this equation in its logarithmic form to the experimental data leads to the values of these constants from the y-intercept and the slope of the following line (Eq. (10)):

$$\ln(q_e) = \ln(K_F) + \frac{1}{n}.\ln(C_e) \tag{10}$$

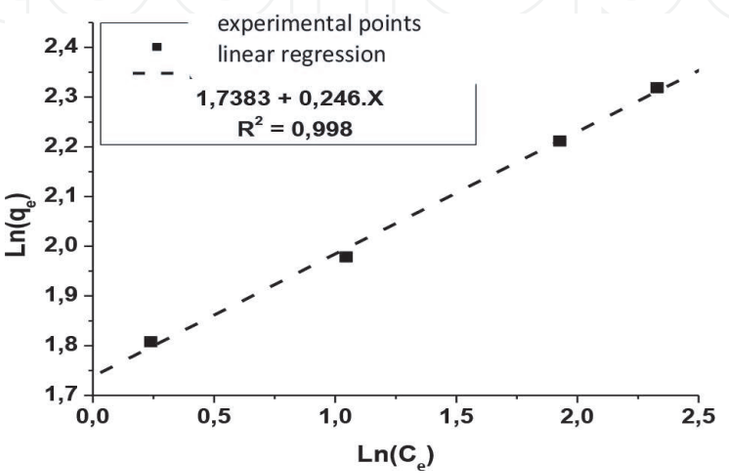


Figure 15.
Freundlich isotherm for the adsorption of phenol on BTC.

Figure 15 shows the obtaining of a perfect line with a correlation coefficient very close to 1 (R^2 = 0.998), for the initial concentrations used, between 10^{-3} M and 6.10^{-3} M. The values found for the constants KF and n are, respectively, equal to 5.68 mg / g and 4.06. The low value of (1 / n = 0.246), indicates that the Freundlich model is more suitable for describing the adsorption isotherm of phenol on a BTC surface having very heterogeneous sites, the number of which is low if the value of KF is taken into account.

4. Conclusion

The study of the adsorption of phenol on commercial BTC has shown that this pollutant can be eliminated from liquid effluents with a fairly large percentage (40%). This encouraging result allows us to extend this study to real industrial discharges. The treatment of bentonite with concentrated HCl (3 N) and (12 N) did not give satisfactory results, although it led to an increase in the specific surface from 35 m^2/g for bentonite not treated to 96 m^2/g for bentonite treated with acid. This is due to a decrease in the number of phenol adsorbing sites and the decrease in the pore diameters as shown by the analyzes by BET and SEM. The modeling of the experimental results of the adsorption isotherm made it possible to specify the most appropriate kinetic model, the adsorption is fast before two hours. It is the Freundlich model which is favorable for a surface having heterogeneous sites. The adsorption capacity was evaluated at 5.68 mg/g. The mechanism of phenol adsorption by hydrogen bonding has also been proven by spectroscopic analyzes. This bond, characterized by the band at 3225 cm^{-1}, results from an interaction between phenol and the free oxygen doublet of the surface.

Author details

Kali Abderrahim, Loulidi Ilyasse, Amar Abdelouahed, Boukhlifi Fatima*, Hadey Chaimaa, Jabri Maria and Mbarka Ouchabi
Laboratory of Chemistry-Biology Applied to the Environment, Faculty of Sciences, Moulay Ismail University, Meknes, Morocco

*Address all correspondence to: f.boukhlifi@umi.ac.ma

IntechOpen

© 2021 The Author(s). Licensee IntechOpen. This chapter is distributed under the terms of the Creative Commons Attribution License (http://creativecommons.org/licenses/by/3.0), which permits unrestricted use, distribution, and reproduction in any medium, provided the original work is properly cited. CC BY

References

[1] Melnitchenko A, Thompson JG, Volzone C, Ortiga J. Selective gas adsorption by metal exchange d amorphous kaolinite derivatives. Applied Clay Science. 2000;**17**:35-53

[2] Dultz S, Bors J. Organophilic bentonite as adsorbents for radionuclides II. Chemical and Mineralogical Properties of HDPY-montmorillonite. Applied Clay Sciences. 2000;**16**:15-29

[3] Hennig BC, Reich T., Dahn R., Scheidegger AM. Structure of uranium sorption omplexes at montmorillonite edge sites. Radiochem. 2002; Acta 90, 653-657.

[4] Bojemueller E, Nennemann A, Lagaly G. Enhanced pesticide adsorption by thermally modified bentonites. Applied Clay Science. 2001;**18**:277-284

[5] Zohra Dali-Youcefa, Hassiba Bouabdasselema, Nourredine Bettaharb, Élimination des composés organiques par des argiles locales, Comptes Rendus Chimie, 2006;**9**(10):1295-1300.

[6] Sprynskyy M. Tomasz Ligor, Kinetic and equilibrium studies of phenol adsorption by natural and modified forms of the clinoptilolite. Journal of Hazardous. 2009;**169**:847-854

[7] Fuqiang Year Baojiao Gao adsorption mechanism and property of novel composite material PMAA / SiO2 Towards phenol, Chemical Engineering Journal 153 (2009) 108-113.

[8] Yu Fei Tao, Wei Gang Lin, Low-cost and effective phenol and basic dyes trapper derived from the porous silica coated with hydrotalcite gel, Journal of Colloid and Interface Science 358 (2011) 554–561.

[9] A. Amar, I. Loulidi, A Kali, F BoukhlifI,1C. Hadey, M. Jabri, Physicochemical Characterization of Regional Clay: Application to Phenol Adsorption", Applied and Environmental Soil Science Volume 2021, ID 8826063 | https://doi.org/10.1155/2021/8826063

[10] Yapar S, Yilmaz M. Removal of Phenol by Using Montmorillonite, Clinoptilolite and Hydrotalcite. Adsorption. 2005;**10**:287-298

[11] Feng Zhen, Structure and properties of hectorite synthesized by microwave and its application, BioChem-Engineering Department, Jiangsu Food College,Jiangsu Huai′an 223001,China.

[12] Ilyasse Loulidi, Fatima Boukhlifi, Mbarka Ouchabi, Abdelouahed Amar, Maria Jabri, Abderahim Kali, and Chaimaa Hadey, Assessment of Untreated Coffee Wastes for the Removal of Chromium (VI) from Aqueous Medium, International Journal of Chemical Engineering, Volume 2021, 11 pages.

[13] Polata H, MolvabM M. Polatc. Capacity and mechanism of phenol adsorption on lignite, International journal of mineral processing. July 2006; **79**(4):264-273

[14] Wen Ping Cheng, Wei Gao, Xinyu Cui, Jing Hong Ma, Rui Feng Li, Phenol adsorption equilibrium and kinetics on zeolite X/activated carbon composite, Journal of the Taiwan Institute of Chemical Engineers, Volume 62, 2016,

[15] Boukhlifi F., Chraibi S, Alami M, "Evaluation of the adsorption kinetics and equilibrium for the potential removal of phenol using a new biosorbent ", Journal of Environment and Earth Science Vol. 3, No. 7. 2013.

[16] Boukhlifi F, Bencheikh A, Ahlafi H. Characterization and adsorption propriety of chitin toward copper Cu^{2+}. Physical and Chemical News. 2011;**58**: 67-72

[17] Boukhlifi F: characterization and treatment of real wastewater from an electroplating company by raw chitin. In: Basheer Al-Naib editor. Book chapter: Recent Advancements in the Metallurgical Engineering and Electrodeposition 2020, Intechopen ISBN 978-1-78984-687-4.

[18] Boukhlifi F: New Approaches and Recent Advances sustainable treatment of heavy metals by adsorption on raw chitin. In: Dr. Mario Alfonso Murillo-Tovar editors, Chapter in book: Trace Metals in the Environment, 2020Intechopen. ISBN 978-1-83880-332-2.

[19] Uday F. Alkaram, Abduljabar A. The removal of phenol from aqueous solutions by adsorption using surfactant-modified bentonite and kaolinite, Journal of Hazardous Materials 169 (2009) 324–332.

[20] Jin S. Hong-fu Lin, Adsorption of phenol from aqueous solutions by organomontmorillonite. Desalination. 2011;**269**:163-169

[21] Richards S, Bouazza A. Phenol adsorption in organo-modified basaltic clay and bentonite. Applied Clay Science. 2007;**37**:133-142

[22] Ma J, Zhu L. Removal of phenols from water accompanied with the synthesis of organobentonite in a one-step process. Chemosphere. 2007;**68**: 1883-1888

[23] Yun-Hwei Shen, Removal of phenol from water by adsorption–flocculation using organobentonite, Water Research 2002;**36**:1107-1114

[24] Hasan Basri Senturk, Duygu Ozdes, Removal of phenol from aqueous solutions by adsorption onto organomodified; Tirebolu bentonite: Equilibrium, kinetic and thermodynamic study, Journal of Hazardous Materials 172 (2009) 353–362.

[25] M. Boufatit, H. Ait -Amar, Development of an Algerian material montmorillonite clay. Adsorption of phenol, 2-dichlorophenol, and from aqueous solutions onto montmorillonite exchanged with transition metal complexes Desalination 206(2007) 394-406.

[26] SYuening Liu, Manglai Gao ∗, Zheng Gu, Zhongxin Luo, Yage Ye, Laifu Lu, Comparison between the removal of phenol and catechol by modified montmorillonite with two novel hydroxyl-containing Gemini surfactants, Journal of Hazardous Materials 267 (2014) 71– 80.

[27] Boukhlifi F. Study of the retention of metallic micro-pollutants (Pb, Cd, Cu, and Zn) on new biosorbent materials: purification tests of liquid industrial effluents, doctoral thesis. Morocco: Chouaib Doukkali El university Jadida; 2000

[28] Greesh N, Hartmann PC, Cloete V, Sanderson RD. Colloid and Interface Science. 2008;**319**:2-11

[29] Busca G, Montanari T, Bevilacqua M, Finocchio E. Inorganic Solids Colloids and Surfaces A: Physicochem. Eng. Aspects. 2008;**320**:205-212

[30] Lagergren, S, K. Svenska. Vetenskapsad. Handl. 24,1 (1898).

[31] Ho. G. McKay. Sorption of dye from aqueous solution by peat, Chem.Eng J. 70 ((1998115–124.

[32] Boukhlifi F, El Akili C, Moussout H, Benzakour A, Ahlafi H. Treatment of Global Rejection of Electroplating Industry by Raw Chitin. Int. J. Appl. About. Sci. 2013;**8**:13-23

[33] Boukhlifi F, Amar A., Loulidi I, Jabri M, Benzakour, A, purification of the waste water of the galvanoplasty industry by natural adsorbents: current Rinsing, RHAZES: Green and

Applied Chemistry Vol 2, 8, 2018, pp.81∼91.

[34] Loulidi I., Boukhlifi F, Ouchabi M., Amar A, Jabri M, Kali, Adsorptive Removal of Chromium (VI) using Walnut Shell, Research Journal of Chemistry and Environment, Vol. 23 (12) December (2019).

[35] Boukhlifi F., Bencheikh A., Study of the competitive adsorption of heavy metals on raw chitin: application to wastewater from the chemical industry. The Water Tribune, N ° 611/3, vol. 55, pp. 37-43, 2001.

[36] Boukhlifi F., Allali M., Bencheikh A., Study of the metallic pollution of wastewater from the chemical industry and test of treatment with crude chitin, Mar. Life, 11 (1-2), pp: 49-56. 2001.

IntechOpen